The correction of diurnal effects on CSTAR photometry

2014 Res. Astron. Astrophys. 14 345

(http://iopscience.iop.org/1674-4527/14/3/008)

RAA 2014 Vol. **14** No. **3**, 345–356 doi: 10.1088/1674–4527/14/3/008
http://www.raa-journal.org *http://www.iop.org/journals/raa*

Research in Astronomy and Astrophysics

The correction of diurnal effects on CSTAR photometry *

Song-Hu Wang[1], Xu Zhou[2], Hui Zhang[1], Ji-Lin Zhou[1], Hui-Gen Liu[1], Ze-Yang Meng[1], Jun Ma[2], Tian-Meng Zhang[2], Zhou Fan[2] and Hu Zou[2]

[1] Department of Astronomy & Key Laboratory of Modern Astronomy and Astrophysics in Ministry of Education, Nanjing University, Nanjing 210093, China
[2] National Astronomical Observatories, Chinese Academy of Sciences, Beijing 100012, China; *zhouxu@bao.ac.cn*

Received 2013 April 11; accepted 2013 November 1

Abstract In January, 2008 the Chinese Small Telescope ARray (CSTAR) was successfully deployed at Dome A, Antarctica. Because CSTAR consists of four static 14.5 cm telescopes pointing at the same $4.5^\circ \times 4.5^\circ$ field around the south celestial pole, diurnal motion can be seen in its field of view. The stars are centered at different positions in different exposure frames. During four months of continuous observations during the polar night of 2008, about 0.3 million i-band images were obtained. In the latest version of the released photometric catalog, the effects of diurnal motion of the stars on the static CSTAR optical system can be obviously found. In this work, we update the CSTAR catalog by carefully analyzing and correcting the systematic errors caused by diurnal motion of stars on imperfectly flat-fielded frames.

Key words: methods: data analysis — techniques: photometric

1 INTRODUCTION

Uninterrupted time-series stellar photometry with high precision, wide field and long baseline can significantly contribute to a large range of astrophysical problems, such as the search for transiting exoplanets, the study of low-level stellar variability and microlensing events (Everett & Howell 2001). Ordinary ground based photometry is not completely adequate for this kind of study as the measurements will be interrupted by daytime and distorted by the atmosphere. One of the most effective solutions is to develop an ambitious space based program such as *CoRoT* (Boisnard & Auvergne 2006) and *Kepler* (Borucki et al. 2010). However, the Antarctic Plateau offers a potentially comparable alternative with significantly lower costs.

Thanks to its extremely cold, dry, calm atmosphere and the thin turbulent surface boundary layer, as well as the absence of light and air pollution, together with the long polar night during winter in the southern hemisphere, the Antarctic Plateau provides an unmatched opportunity for ground based telescopes to obtain continuous high-quality time-sampled photometric sequences (Burton 2010).

Dome A, located far inland in Antarctica, is about 1200 km from the Chinese Zhongshan station. With a surface elevation of about 4093 m, it is the highest astronomical site in Antarctica. After comparing with other Antarctic sites in terms of weather, boundary layer, airglow, aurorae, precipitable

* Supported by the National Natural Science Foundation of China.

water vapor, surface temperature, thermal sky emission and free atmosphere, Saunders et al. (2009) declared that Dome A might be the best site on Earth for acquiring astronomical data.

In order to take advantage of observational conditions at Dome A, in January, 2008 the Chinese Small Telescope ARray (CSTAR) was shipped and deployed there to undertake both site testing and science research tasks. With high-cadence automatic observations, about 0.3 million qualified i-band CCD images were acquired during the Antarctic winter of 2008.

Based on these images, the first version of the CSTAR point source catalog has been released (Zhou et al. 2010a) and was recently updated (Wang et al. 2012) when the inhomogeneous effects of extinction over the large CSTAR field of view (FOV) were carefully considered. Data from CSTAR have also been successfully used to test the site characteristics of Dome A (Zou et al. 2010) and search for variable stars (Wang et al. 2011).

Thanks to these photometric sequences that have high quality and high time resolution, data from CSTAR can be also used to search for signals of transiting exoplanets. Using the transit method to detect exoplanets requires photometry with precision significantly better than the typical depth of a transit for a Jupiter-sized planet ($\sim$0.01 mag). Successful transit surveys typically achieve photometric precisions of 0.005 mag or better (e.g. *HAT*: Bakos et al. 2007, *WASP*: Pollacco et al. 2006), but the current CSTAR catalog (Wang et al. 2012) cannot completely meet this requisite precision.

To further improve the photometric accuracy of CSTAR data, we have carefully analyzed potential systematic errors affecting the photometric accuracy. In addition to the corrected effects of the unevenness of extinction across the large CSTAR FOV (Wang et al. 2012), several kinds of possible systematic errors remain, such as ghost images, undersampling of the CCD, and systematic diurnal changes in the brightness of stars during their daily circular motion around the south celestial pole on the static CSTAR optical system. In this work, we focus on analyzing and correcting the diurnal effects caused by the combination of the diurnal motion of stars and the non-flat photometric images. Other systematic errors will be corrected in future work.

A common technique of photometric calibration performed within an ideally flat-fielded image can lead to very good accuracy. However, while a night-sky super flat field and a residual flat field have been applied (Zhou et al. 2010a), flat-field corrections of CSTAR data have still been found to be unsatisfactory. The imperfect nature of flat-field calibrations can result in spatially dependent errors which show up as daily variations when the stars are centered on different pixels in different exposure frames during their diurnal motion around the south celestial pole on the static CSTAR optical system. As a result, it will lead to an increase in the noise of light curves, or worse still, will produce strong false diurnal signals, which will hide extremely weak transiting signals that we are trying to search for.

Fortunately, because CSTAR is a static telescope pointing at the south celestial pole without any moving parts, the stars in the neighboring diurnal circles travel similar daily paths on the CCD and suffer similar effects of spatially dependent systematic errors. Therefore, for each of the stars within the CSTAR FOV, one of the most stable stars with high photometric precision in a nearby diurnal circle can be selected as the reference star to look for a residual flat-field pattern in the path taken on the CCD. This pattern can then be used to correct the systematic diurnal variations of the object that we focus on. We update the CSTAR catalog by removing these systematic diurnal variations of all the stars within the CSTAR FOV in this way.

The layout of the paper is as follows. In Section 2 we describe the instruments, observations and previous data reduction of CSTAR images. The characteristics and causes of diurnal effects on CSTAR photometry are analyzed in Section 3. In Section 4, we give the method for updating the CSTAR catalog by correcting the false diurnal signals in it. Then, we carefully analyze and discuss our method and results in Section 5. Finally, the work is summarized in Section 6.

2 INSTRUMENTS, OBSERVATIONS AND PREVIOUS DATA PROCESSING

2.1 CSTAR Instruments

CSTAR is an array of four identical, static Schmidt telescopes with the same $4.5^\circ \times 4.5^\circ$ FOV directed toward the south celestial pole. The four telescopes have different filters respectively listed as SDSS bands g, r, i and open. Each telescope gives a 145 mm entrance pupil diameter (effective aperture of 100 mm) and has a $1\,\mathrm{k} \times 1\,\mathrm{k}$ Andor DV 435 frame transfer CCD array, with a pixel size of $13\,\mu\mathrm{m}$ and plate scale of $15\,\mathrm{arcsec\,pixel}^{-1}$. As the first Chinese telescope based in Antarctica, CSTAR was designed to be totally fixed, without any moving parts. More details of the instruments on CSTAR are presented in Zhou et al. (2010b).

2.2 Observations

In January, 2008 after being effectively and extensively tested (Zhou et al. 2010b), CSTAR was shipped and deployed at Dome A. Although some problems prevented us from obtaining useful data in the g, r and the open bands, fortunately, in the i band, the observations were successfully conducted from 2008 March 4 to August 8. About 0.3 million qualified images were obtained with 20-second exposure times. There were about 1728 hours of exposure time in total. In good photometric conditions, more than 10 000 sources down to $i = 16$ could be detected. Similar observations were acquired over the last five years. Our current work is based on the data from 2008. The details of the observations in 2008 are presented in Zhou et al. (2010a).

2.3 Previous Data Processing

After obtaining high quality images from the CSTAR telescope in 2008, the first version of the catalog of all the point sources within the CSTAR FOV was released by Zhou et al. (2010a) and recently updated (Wang et al. 2012) when the inhomogeneous effects of extinction over the large CSTAR FOV were carefully considered.

We briefly review the previous data processing techniques here. In the work Zhou et al. (2010a), because there is no real-time flat field, a super flat field, derived from the median combination of the images taken under conditions of high sky background, after removal of the stars using sigma clipping, was first applied to all of the CSTAR images. Then, a 'residual flat field' image was constructed and applied according to systematic changes in the brightness of stars during their diurnal motion around the south celestial pole. After preliminary reduction, aperture photometry was conducted to derive the instrumental magnitudes of over 10 000 stars that were typically identified in each of the 300 000 CSTAR images. After the magnitudes had been flux calibrated to the USNO-B 1.0 photometric system by the 48 brightest stars within the CSTAR FOV, the first version of the CSTAR catalog, detailed in Zhou et al. (2010a), was released.

To produce another CSTAR catalog with higher precision, we have corrected the unevenness of extinction across the large CSTAR FOV. We compared an ensemble of differences in the detected magnitudes of the bright and unsaturated stars in the first version of the catalog (Zhou et al. 2010a) with their magnitudes in the reference catalog (Wang et al. 2012) which contains the mean magnitude of every star within the CSTAR FOV. With the obtained distribution of magnitude differences (which infer the structure of uneven extinction), we corrected and updated the CSTAR catalog from 2008. More details are given in Wang et al. (2012).

3 THE CHARACTERISTICS OF DIURNAL EFFECTS ON CSTAR DATA

The Box-fitting Least Squares (BLS) algorithm (Kovács et al. 2002) is a widely used method for light curve analysis. When it is implemented for computing periodograms of the light curves from the released CSTAR data, a similar diurnally-dominate periodic pattern, as shown in Figure 1, appears.

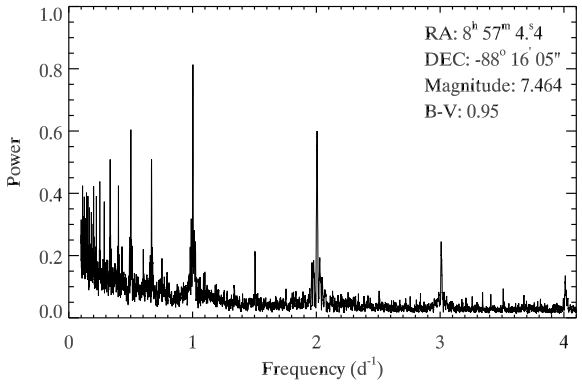

Fig. 1 An example of a normalized BLS periodogram of a light curve from the released CSTAR data. Parameters describing the star are shown in the upper right corner of the panel. The color index of the star is derived from Tycho-2 $B - V$ (Høg et al. 2000). The star is 1.75° (420 pixels) away from the south celestial pole. The significant diurnally-dominate periodic pattern in the periodogram is considered to be an artifact.

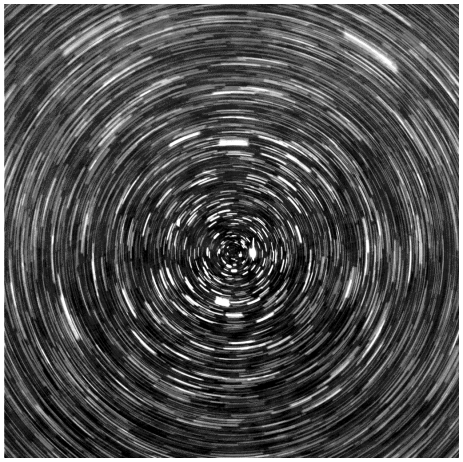

Fig. 2 The concentric diurnal trails traced by objects observed by CSTAR during one-hour frames. Because CSTAR is a static telescope pointing toward the south celestial pole without any moving parts, stellar diurnal motion can be seen from consecutive frames. The stars are centered at different positions in different exposure frames. The diurnally-dominate periodic pattern in every light curve of CSTAR is thought to be entirely due to the diurnal motions of these objects observed by CSTAR on imperfectly flat-fielded frames.

This kind of diurnally-dominate periodic pattern, existing in the periodograms of every CSTAR time series, is considered to be an artifact. Because CSTAR is a static telescope pointing toward the south celestial pole without any moving parts, the objects produce concentric diurnal motions (Fig. 2) on the frames of CSTAR. The stars are centered on different positions in different frames. After careful analysis, the diurnally-dominate periodic pattern is thought to be entirely due to the diurnal motion of objects observed by CSTAR on imperfectly flat-fielded frames, which leads to spatially dependent errors. Three of the most representative analysis results are given as follows.

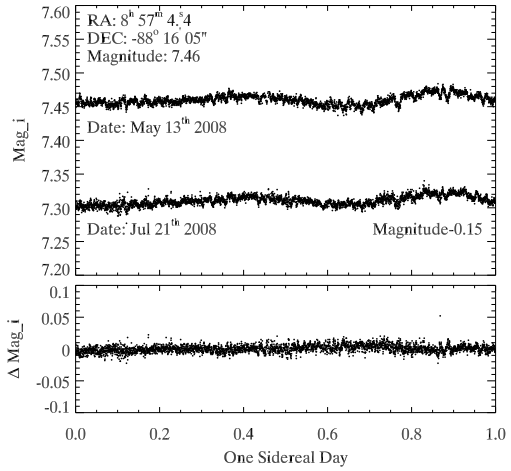

Fig. 3 Two parts of the light curve of the same star on different days are shown in the upper panel. The lower light curve is offset by 0.15 mag for clarity. The difference between these two parts of the light curve is shown in the lower panel. Clearly, the structure of two parts of the light curve is similar and almost unchanged, although they are taken more than two months apart.

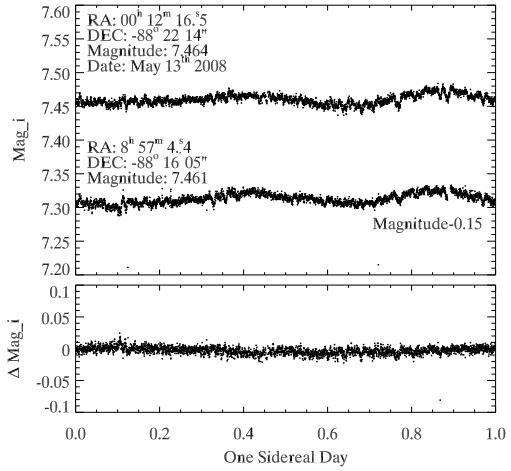

Fig. 4 Same as Fig. 3, but for two stars with similar distances from the pole. Clearly, the stars with a similar distance from the pole, traveling on neighboring diurnal circular paths on the CCD, suffer similar systematic effects.

(1) As shown in Figure 3, the same star within the CSTAR FOV, traveling the same circular path on the CCD during its daily motion on different days (strictly known as a sidereal day), shows a similar diurnal signal. Although taken more than two months apart, the structure of the light curves from the star is almost unchanged. This is the first strong evidence for our consideration to only ascribe this kind of diurnal signal to spatially dependent errors in the non-flat scientific frames and the diurnal motion of the stars on the static telescope.

(2) As shown in Figure 4, two stars with similar distances from the pole show a similar diurnal signal when they travel on neighboring circular paths on the CCD. This is yet another exam-

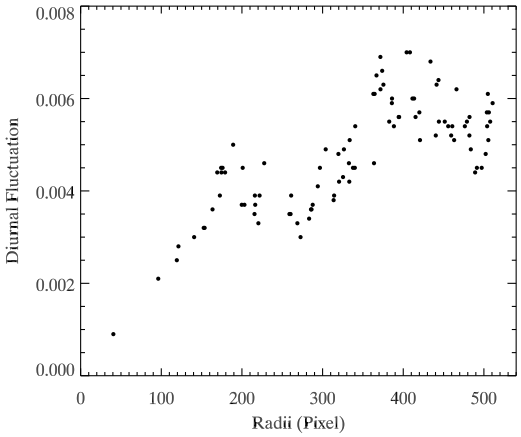

Fig. 5 The relationship between the systematic diurnal fluctuation of the stars and their distance from the pole in pixels. Each point represents the systematic fluctuation of a stable CSTAR object with high photometric precision. From the figure we can find that the systematic diurnal fluctuation of a star roughly increases with its distance from the pole or the number of pixels the star passes. The systematic diurnal change of a star traces the residual flat-field structure of the CCD path the star follows. The more pixels the star passes, the more likely it is to be affected by the residual flat-field structure. It is worth noting that some stellar paths may be longer, but their paths are more smooth. For that reason, some have a larger distance from the pole but less diurnal fluctuation.

ple demonstrating that similar systematic errors will affect stars in neighboring diurnal cycles. Together with the first example, the pattern of diurnal effects on CSTAR data provides guidance on how we can remove these effects.

(3) The other example that demonstrates the effects of spatially dependent calibration errors combined with diurnal motion of stars is shown in Figure 5, where the systematic diurnal changes of the stars roughly increase with their distance from the pole or with the number of pixels that the stars pass. The maximum systematic diurnal change of the star goes up to 0.007 mag. This periodic signal hides the smaller signals needed for detecting transiting planets, thus hindering the search process.

4 THE CORRECTION OF DIURNAL EFFECTS

Based on the analysis above, stars in neighboring daily circles suffer similar effects of spatially dependent systematic errors during their diurnal motion on similar CCD paths. For that reason, the diurnal effects on each object observed by CSTAR can be removed by comparing it with a proper reference star in a nearby diurnal circle.

The step by step process of correcting diurnal effects on objects observed by CSTAR is shown below:

(1) *The light curve of the target object.*
The light curve of the target object that needs correcting can be denoted by $\{\mathrm{mag}_i, t_i\}$. As we are only concerned about the diurnal effects in the light curve, when given a zero point for and the period of one sidereal day, the time-magnitude light curve of the target object can be converted to a phase-magnitude light curve: $\{\mathrm{mag}_{\tilde{i}}, \phi_{\tilde{i}}\}$, where $\{\tilde{i}\}$ is a permutation of $\{i\}$.

(2) *The selection of the reference star.*
As shown in Figure 6, in order to find the pattern of systematic changes of the diurnal path taken by the target object on the CCD (filled circle), the brightest unsaturated star ($7.5 < \mathrm{mag}_i <$

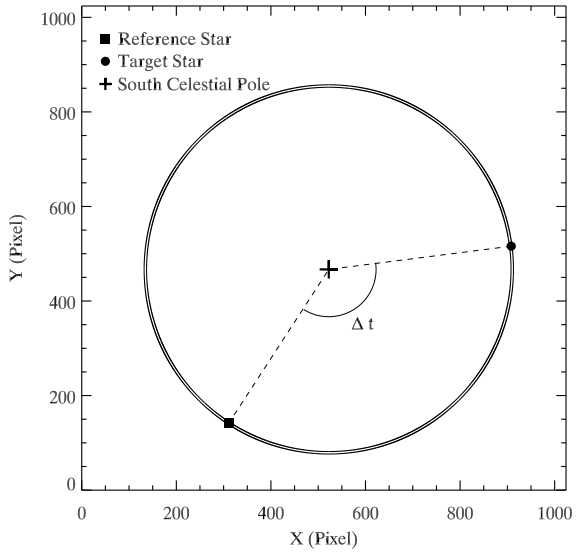

Fig. 6 The schematic of the target star and reference star from the example demonstrating our method. In traditional differential photometry, the reference star is selected from nearby stars. In our specific differential approach, to correct the diurnal effects in the light curve caused by the residual flat field, the reference star can be selected from all the stars on a similar diurnal path as the target star. As the figure shows, the two stars travel a similar diurnal path on the CCD and therefore suffer similar diurnal effects on the residual flat field. For that reason, when a phase offset (Δt) was applied to the time-series of the reference star, it can be used to correct the diurnal effects in the light curve of the target star.

10.5) traveling on a nearby diurnal path on the CCD (less than 5 pixels) with constant brightness is selected as the reference star (filled square). We denote the light curve of the reference star by $\{\mathrm{mag}_{0j}, t_{0j}\}$, and each mag_{0j} includes additive photometric noise with standard deviation σ_{0j}. The effect of noise is mitigated by assigning a weight ω_{0j}, defined as $\omega_{0j} = \sigma_{0j}^{-2}$, to each data point.

(3) *The time shift of the light curve from the reference star.*
As shown in Figure 6, although these two stars (the target object and the reference star) travel on neighboring circular paths on the CCD, at the same time two stars fall on a different phase of the circle because of their different right ascensions. To establish the same time-position relation for these two stars, a time shift ($\Delta t = \mathrm{RA} - \mathrm{RA}_0$) — directly derived from the difference in right ascension between the target object (RA) and the reference star (RA_0) — is applied to the light curve of the reference star by $\tilde{t}_{0j} = t_{0j} + \Delta t$, where $\tilde{t}_{0j}$ represents the shifted sampling time of the light curve from the reference star, and t_{0j} refers to the original sampling time of the light curve from the reference star. The time-shifted light curve of the reference star is denoted by $\{\mathrm{mag}_{0j}, \tilde{t}_{0j}\}$.

(4) *The magnitude shift of the light curve of the reference star.*
We want to obtain the corrected magnitude of the object in an absolute manner. Therefore, we subtract the mean magnitude from the light curve of the reference star. The magnitude-shifted light curve of the reference star, with an average magnitude of nearly zero, is denoted by $\{\widetilde{\mathrm{mag}}_{0j}, \tilde{t}_{0j}\}$.

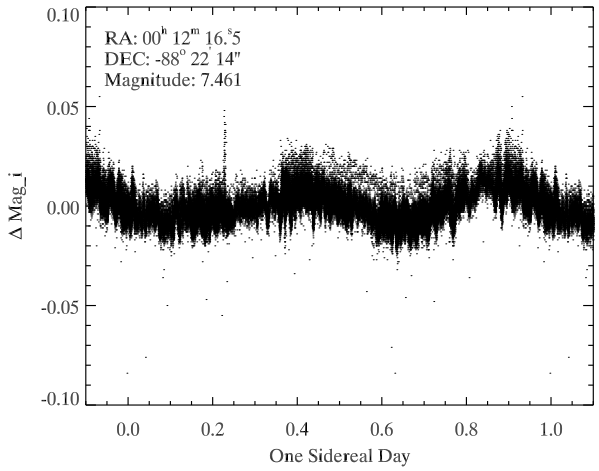

Fig. 7 The reference star, with high photometric precision and constant brightness, is selected to find the pattern of diurnal variations for the correction to the CCD path taken by the target object of the example. For a given zero point of time and a given period (one sidereal day), the folded light curve of the reference star, shown by the light points, was obtained to form the average light curve (*denoted by the dark line*), which has high signal-to-noise ratio after the correction.

(5) *The folded light curve of the reference star.*
The traditional way of doing differential photometry is to directly compare the target star with the reference star over the whole observing span. We are only concerned about the diurnal effects in the light curve. The average one-day folded light curve of a reference star has an extremely high signal-to-noise ratio, which will result in more reliable corrected data. The method to produce the high-precision reference light curve is covered in this step and steps 6 and 7.

For the zero-point and the period to be the same as those that are applied to the light curve of the target object in step 1, a folded time series from the reference star, shifted by steps 3 and 4, is obtained and denoted by $\{\widetilde{\mathrm{mag}}_{0\tilde{j}}, \phi_{0\tilde{j}}\}$. Each point has a weight $\omega_{0\tilde{j}}$, where $\{\tilde{j}\}$ is a permutation of $\{j\}$. The folded light curve of the reference star in the example is shown in Figure 7 by the light points.

(6) *The bins of the folded light curve of the reference star.*
We divide the folded time series of the reference star into k bins, where $k = [1.429 \times r]$. The constant (1.429) is an optimized scale for correction, r is the radius of the diurnal circle of the reference star in pixels and square brackets are used to denote the floor function. This approach is very computationally efficient and yields a proper frequency structure of the residual flat field for the circular path on the CCD that we focus on. Both the additional high-frequency noise and the unsatisfactory correction with excessively low frequency are avoided.

(7) *The weighted average magnitude for bins.*
For any given bin, the weighted average magnitude of all the points in this bin can be evaluated by

$$\overline{\mathrm{mag}}_l = \frac{\sum \widetilde{\mathrm{mag}}_0 \cdot \omega_0}{\sum \omega_0}. \tag{1}$$

The weighted average light curve can be denoted by $\{\overline{\mathrm{mag}}_l,\ \theta_l\}$, where θ_l, the phase of each bin, can be determined by $\theta = \frac{l}{k}$, where k is the total number of bins, and l is the index of the bin we focus on. The weighted average light curve of the reference star in the example is denoted by the dark line in Figure 7.

(8) *The correction of the original light curve.*
For each point in the light curve of a target object in the phase-magnitude form, $\{\mathrm{mag}_{\tilde{i}}, \phi_{\tilde{i}}\}$, we can evaluate a correction value by a linear interpolation between $\{\overline{\mathrm{mag}}_l, \theta_l\}$ and $\{\overline{\mathrm{mag}}_{l+1}, \theta_{l+1}\}$ $(\theta_l \leq \phi_{\tilde{i}} \leq \theta_{l+1})$

$$\delta\mathrm{mag}_{\tilde{i}} = \overline{\mathrm{mag}}_l + \frac{\overline{\mathrm{mag}}_{l+1} - \overline{\mathrm{mag}}_l}{\theta_{l+1} - \theta_l} \cdot (\phi_{\tilde{i}} - \theta_l), \tag{2}$$

where $\delta\mathrm{mag}_{\tilde{i}}$ is the value for correction of the $\tilde{i}^{\mathrm{th}}$ point in the phase-magnitude light curve of the target object. We can correct each point in the light curve by each obtained $\delta\mathrm{mag}_{\tilde{i}}$.

In this way, all the light curves extracted from the released CSTAR catalog can be corrected and then converted to a new version of the catalog.

5 RESULTS AND DISCUSSION

The main focus of this work concentrates on improving the photometric precision of the previously published CSTAR catalog (Wang et al. 2012) by removing systematic errors caused by the diurnal motion of stars on the static CSTAR optical system without a perfect flat field. Thus, here we compare the light curves from the previously published CSTAR catalog and the revised catalog to show the effects of correction.

First of all, the BLS spectra computed from a light curve is presented in Figure 8 that is corrected for diurnal effects of the same star as in Figure 1. The star is 1.75° (420 pixels) away from the south celestial pole with $i = 7.46$. An identical normalized standard is applied to these two BLS spectra. Compared with Figure 1, the diurnally-dominate periodic pattern in Figure 8 derived from the revised light curve does not completely disappear, but has much weaker power.

Subsequently, as shown in Figure 9, we compare two light curves of the above-mentioned star during a one-day interval on 2008 May 13. The upper light curve is that from the previously published catalog (Wang et al. 2012). There is distinct fluctuation in magnitude in the light curve. The root mean square (r.m.s.) scatter of this part of the light curve is 0.0073. The lower one is the light curve from our newly revised catalog with r.m.s. of 0.0034. It is clear that the distinct diurnal structure in the original light curve has been completely removed. The photometric precision of the light curve has been significantly improved.

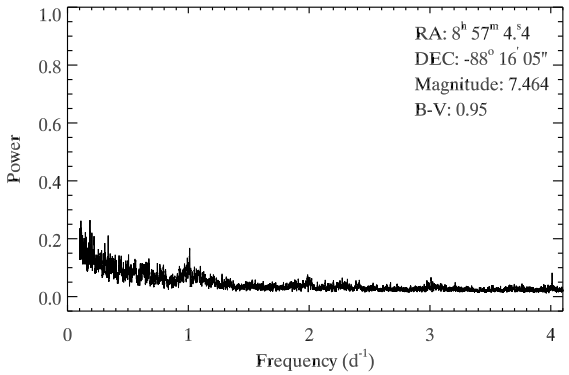

Fig. 8 The BLS spectra computed from a light curve with correction for diurnal effects of the same star in Fig. 1. Compared with Fig. 1, the diurnally-dominate periodic pattern does not completely disappear, but it has much weaker power after the correction.

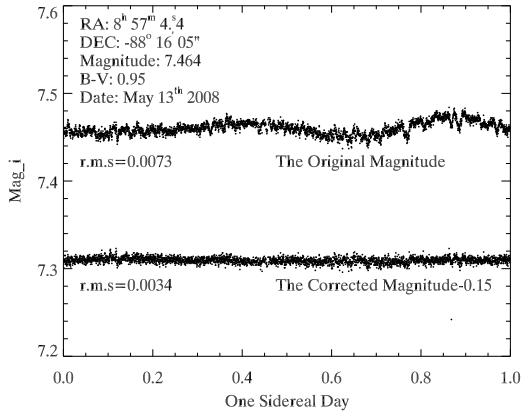

Fig. 9 The before and after comparison of correction for the diurnal effects in a light curve. The corrected light curve is offset by 0.15 mag for clarity. The obvious diurnal structure in the original light curve has been completely removed. The precision of the light curve taken with CSTAR has been significantly improved.

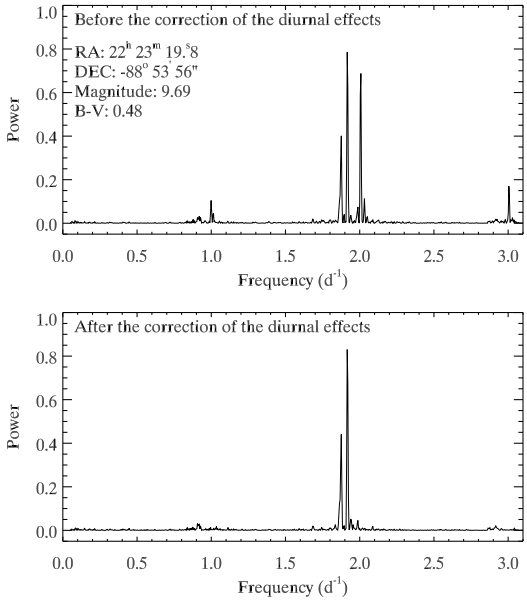

Fig. 10 Comparison of the Lomb-Scargle spectra computed from the light curve of a pulsating variable star before and after correction. The periodogram of the revised light curve clearly shows the periodic structure of the γ Doradus variable star. It is no longer subject to harmonic disturbances in diurnal frequency.

Furthermore, to show how the correction of diurnal effects helps in detecting more frequencies in light curves taken with CSTAR, an example of correction applied to a pulsating variable star is shown in Figure 10, which presents a comparison of the normalized Lomb-Scargle periodogram (Zechmeister & Kürster 2009) computed from the light curve of a γ Doradus variable star (Wang et al. 2011) before and after correction. The periodogram of the revised light curve clearly shows

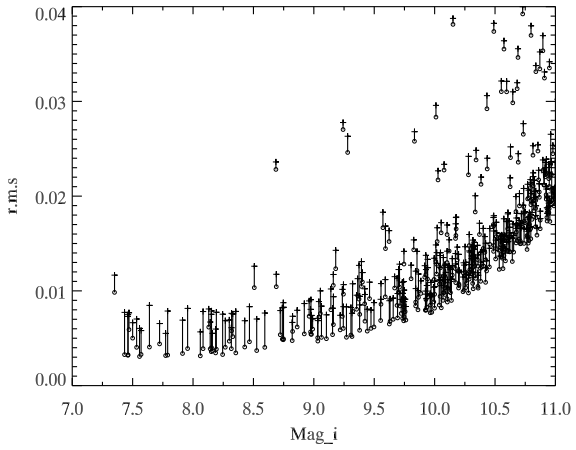

Fig. 11 The standard deviation of the light curves around the reference magnitude of CSTAR. Each '+' or '○' represents a light curve. The '+' symbols refer to the r.m.s. of the original light curves, and the '○' symbols denote the r.m.s. of the final corrected light curves. Each couple of r.m.s. values is connected by a straight line segment. Clearly, the method significantly decreases the r.m.s. value of the light curves.

the periodic structure of the variable star. It is no longer subject to harmonic disturbances in diurnal frequency.

Finally, we show the distribution of r.m.s. values for bright objects observed by CSTAR in Figure 11, where the '+' symbols refer to the r.m.s. of the original light curves, and the '○' symbols show the r.m.s. of the revised light curves. Each '+' or '○' represents a light curve taken over one day. Each couple of r.m.s. values is connected by a straight line segment. Clearly, the correction significantly decreases the r.m.s. value of the light curves. For the brightest unsaturated stars, the resulting light curves typically reach a per-point photometric precision of ~ 4 mmag r.m.s. (or better) around their mean magnitude in the reference catalog. Without this correction, it would be hard for CSTAR to achieve this considering its effective aperture is just 10 cm.

In addition, we also compare our correction method with traditional differential photometry. Differential photometry is the measurement of the brightness of an object relative to one or more nearby comparison stars that have constant brightness, which is a popular solution in photometry that has space-dependent or time-dependent errors. Because the neighboring stars suffer similar spatially dependent systematic errors, traditional differential photometry can also remove the systematic diurnal changes of the objects observed by CSTAR, but cannot achieve the same precision as our method. The most likely reason is that traditional differential photometry is not designed for a specific period as our method is. In our method, the average light curve from hundreds of repeated folded light curves of the reference star will contribute to the reference star with an extremely high signal-to-noise ratio which is unachievable in traditional differential photometry. Furthermore, although multiple comparison stars can average out much of the spatial errors (such as the gradients in the field around the object), traditional differential photometry is mainly designed for removing the low-frequency spatial calibration errors, with little concern for the exact variations in the response of the path that the object travels, which has been carefully accounted for in our method. Additionally, in traditional differential photometry, for some objects, it is difficult to select proper comparison star(s), which should be bright and unsaturated, near the object, and have constant brightness. But in our method, the proper reference stars can be selected from all stars in the same diurnal annulus with the target object, which will contribute to the high-precision correction.

6 SUMMARY AND CONCLUSIONS

In 2008, CSTAR was deployed at Dome A to provide high-cadence photometry during the Antarctic polar night for the purpose of further probing the quality of Dome A and taking advantage of Antarctic photometry to detect types of variable objects, including exoplanetary transiting events.

As CSTAR is a static telescope pointing at the south celestial pole without any moving parts, the residuals of flat-fielded photometric frames are embedded in the light curve of objects during their diurnal motion. Compared with traditional differential photometry, a specific and more effective differential photometry was applied to correct the systematic diurnal change of every object observed by CSTAR: comparing the target with the brightest constant reference star in a nearby diurnal path. The photometric accuracy has been significantly improved; the photometric precision of the brightest unsaturated ($i = 7.5$) stars improved from $\sim$8 mmag to $\sim$4 mmag, which allows an efficient search for variable stars and transit candidates. An updated version of the catalog with higher photometric precision is now available online (*http://archive.bao.ac.cn/en/cstar*).

Acknowledgements This work has been supported by the National Basic Research Program of China (973 Program, No. 2013CB834900), the National Natural Science Foundation of China (Grant Nos. 11073032, 10925313 and 10833001), the National Natural Science Funds for Young Scholar (No. 11003010) and Research Fund for the Doctoral Program of Higher Education of China (No. 20090091120025). We thank Rob Wittenmyer for his help with grammar and expression.

References

Bakos, G. Á., Noyes, R. W., Kovács, G., et al. 2007, ApJ, 656, 552
Boisnard, L., & Auvergne, M. 2006, in ESA Special Publication, 1306, eds. M. Fridlund, A. Baglin, J. Lochard, & L. Conroy, 19
Borucki, W. J., Koch, D., Basri, G., et al. 2010, Science, 327, 977
Burton, M. G. 2010, A&A Rev., 18, 417
Everett, M. E., & Howell, S. B. 2001, PASP, 113, 1428
Høg, E., Fabricius, C., Makarov, V. V., et al. 2000, A&A, 355, L27
Kovács, G., Zucker, S., & Mazeh, T. 2002, A&A, 391, 369
Pollacco, D. L., Skillen, I., Collier Cameron, A., et al. 2006, PASP, 118, 1407
Saunders, W., Lawrence, J. S., Storey, J. W. V., et al. 2009, PASP, 121, 976
Wang, L., Macri, L. M., Krisciunas, K., et al. 2011, AJ, 142, 155
Wang, S., Zhou, X., Zhang, H., et al. 2012, PASP, 124, 1167
Zechmeister, M., & Kürster, M. 2009, A&A, 496, 577
Zhou, X., Fan, Z., Jiang, Z., et al. 2010a, PASP, 122, 347
Zhou, X., Wu, Z.-Y., Jiang, Z.-J., et al. 2010b, RAA (Research in Astronomy and Astrophysics), 10, 279
Zou, H., Zhou, X., Jiang, Z., et al. 2010, AJ, 140, 602